JOURNAL OF APPLIED ELECTROCHEMISTRY 23 (1993) 655–661

Electroformation of electrocatalytically active hydrous oxide layers on a Co–Ni amorphous alloy under pulsating electrolysis*

W. E. TRIACA, A. J. ARVIA

Instituto de Investigaciones Fisicoquímicas Teóricas y Aplicadas (INIFTA), Facultad de Ciencias Exactas, Universidad Nacional de La Plata, Sucursal 4, Casilla de Correo 16, 1990 La Plata, Argentina

T. KESSLER

Facultad de Ingeniería, Universidad Nacional del Centro de la Provincia de Buenos Aires, Casilla de Correo 12, 7400 Olavarría, Argentina

Received 12 March 1992; revised 9 September 1992

A hydrous oxide film can be grown on a $Co_{50}Ni_{25}Si_{15}B_{10}$ amorphous alloy through the application of a periodic perturbing potential routine in alkaline solution. The optimal parameters of the square wave potential signal are determined. The oxide film is a precursor of a Co–Ni spinel as concluded from voltammetry, i.r. spectroscopy, XPS and SEM micrography. The catalytic activity of the oxide layer for the oxygen evolution reaction is demonstrated.

1. Introduction

In the previous ten years new materials for alkaline water electrolysis have been proposed, particularly as efficient anodes for the oxygen evolution reaction (o.e.r.). A number of mixed metal oxides appear very promising for that purpose [1–3], such as the $NiCo_2O_4$ spinel which, in base solutions, exhibits a high activity for the o.e.r., a great resistance to corrosion and a low electrical resistivity [4, 5]. Furthermore, it was also observed that metallic glasses offer several interesting electrocatalytic properties which can be improved through either thermal, chemical or electrochemical treatments [6–13], producing the so-called electrocatalysts with an amorphous precursor [9]. For the latter the origin of the catalytic activity could be due either to the proper amorphous structure, or to the presence of a thin anodic layer on the metal, or to both contributions acting simultaneously. This important matter, however, is not yet definitely clarified.

A Co–Ni amorphous alloy denoted as G16 ($Co_{50}Ni_{25}Si_{15}B_{10}$) has been proposed as a good electrocatalyst for the o.e.r. [14, 15]. The kinetics and mechanism of this reaction in alkaline solution at different temperatures was studied by means of electrochemical impedance spectroscopy (EIS) [16]. Nevertheless, further improvement of the catalytic activity of the Co–Ni amorphous alloy is required for its possible application to practical alkaline fuel cells and electrolysers.

Recently, the formation of a hydrous oxide film at an amorphous Ni–Co alloy by potential cycling was reported [17]. Macroscopic growth of metal hydrous oxide films can also be produced in a reproducible and effective way by triangular potential cycling at low potential sweep rates [18, 19] or through the application of a repetitive square wave potential (RSWP) routine to both polycrystalline (pc) nickel and cobalt electrodes in alkaline solution [20–22]. It is attractive to apply the latter procedure directly to the G16 alloy in attempting to improve the electrocatalytic activity of this material for the o.e.r.

The present paper describes the modification of the Co–Ni amorphous alloy G16 through the formation of a thin oxide layer by applying the RSWP technique in alkaline solution. The resulting oxide layer has been characterized by cyclic voltammetry, IR spectroscopy, XPS, and SEM. Exploratory electrochemical data of the modified G16 alloy for the o.e.r. are also reported.

2. Experimental details

The working electrodes (about 1 cm^2 average total geometric area) were made from the G16 glassy metal alloy ($Co_{50}Ni_{25}Si_{15}B_{10}$) (Vakuumschmelze GmbH, Hanau), and consisted of ribbons of 50 μm thickness. Electrical contact was made at the end of the ribbon by pressing a copper wire, the entire contact being sealed with a Teflon ribbon.

Runs were made at 30 °C in a conventional three electrode cell, using 1 M NaOH, prepared from analytical grade (p.a. Merck) reagent and fourfold distilled water. A large platinized platinum electrode and a reversible hydrogen electrode in the same solution were used as counter electrode and reference electrode, respectively.

* This paper is dedicated to Professor Brian E. Conway on the occasion of his 65th birthday, and in recognition of his outstanding contribution to electrochemistry.

0021-891X

Prior to the experiments the working electrode surface was etched in 50% H_2SO_4 for a few seconds and repeatedly rinsed with fourfold distilled water. Afterwards, reproducible initial voltammograms could be obtained in 1 M NaOH at 0.1 V s^{-1} between 0.05 and 1.55 V.

The repetitive square wave potential (RSWP) treatment consisted of the application of a time-symmetric signal from E_u ($0\,V \leqslant E_u \leqslant 2.0\,V$) to E_l ($-3.0\,V \leqslant E_l \leqslant 0\,V$) at a frequency f ($0.025\,kHz \leqslant f \leqslant 5\,kHz$) during a time t ($10\,s \leqslant t \leqslant 300\,s$). The electrode surface was then stabilized by repetitive triangular potential cycling at 0.1 V s^{-1} between 0.05 and 1.55 V.

The relative increase in the working electrode active surface area was evaluated from the ratio, $R = Q_a/Q_b$, where Q_a and Q_b are the overall voltammetric charges after (a) and before (b) the RSWP treatment, respectively, measured at 0.1 V s^{-1} between 0.05 and 1.55 V. Occasionally, RSWP treated working electrodes were further treated at 380 °C for 2 h under a nitrogen atmosphere.

A 750 Shimadzu spectrometer was used for the XPS analysis. Specimens were irradiated by MgK_α X-rays with a mean energy of 1253.6 eV at low pressure, 10^{-6} Pa. The corresponding spectra were recorded for the O 1 s, Co 2p and Ni 2p binding energies. Unfortunately, the amount of boron could not be determined properly because of its low effective cross section. The XPS spectra were calibrated using the Ag 3 $d^{5/2}$ mean peak at 368.2 eV and taking the C 1s spectra at 284.6 eV as reference.

The composition ratio of the elements (1 and 2) in the film, as given by the n_1/n_2 ratio, was estimated from the corresponding peak areas of the XPS spectra through the following equation:

$$\frac{n_1}{n_2} = \frac{\lambda_2 S_2 I_1 \delta_2}{\lambda_1 S_1 I_2 \delta_1} \qquad (1)$$

where δ_i is the photoelectronic cross section, λ_i is the escape depth in nanometre for $i = 1$ or 2. The parameter λ_i is given by $\lambda_i = 641\,E^{-2} + 0.096E^{1/2}$; E is the kinetic energy, I_i is the intensity of the peaks, and S_i is the sensitivity factor of the apparatus. The latter is related to the binding energy, E_b, through the following expression $S_i = 0.67 + 3.3 \times 10^{-4}E_b$.

Conventional equipment was employed for i.r. spectroscopy, X-ray diffractometry, and SEM experiments.

3. Results

3.1. *Cyclic voltammetry*

The initial voltammogram at 0.1 V s^{-1} for G16 in 1 M NaOH after the chemical pretreatment in 50% H_2SO_4 (Fig. 1a) shows poorly defined anodic–cathodic current peaks, but after approximately 10 min cycling between 0.05 and 1.55 V the stabilized voltammogram (blank) is reached (Fig. 1b). The latter exhibits defined anodic and cathodic peaks at about 1.3 V, and 1.2 V, respectively.

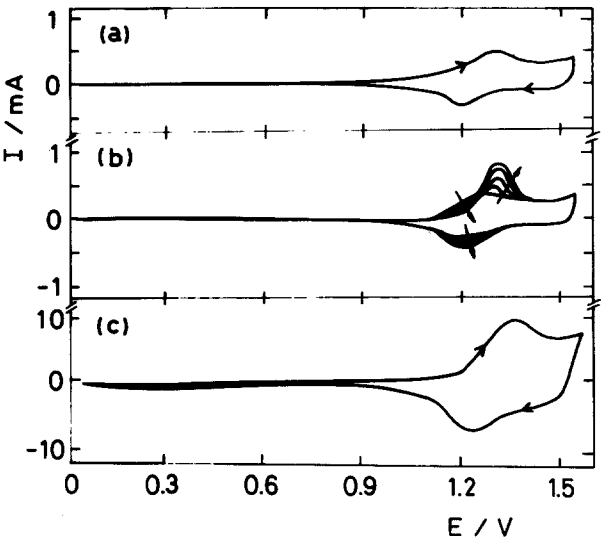

Fig. 1. Voltammograms for a G16 sample run at 0.1 V s^{-1} in 1 M NaOH, 30 °C. (a) First sweep and (b) successive profiles after the chemical treatment, (c) stabilized profile after the RSWP treatment ($E_u = 1.0\,V$, $E_l = -1.0\,V$, $f = 0.6\,kHz$, $t = 1\,min$).

After the RSWP treatment ($E_u = 1.0\,V$, $E_l = -1.0\,V$, $f = 0.6\,kHz$, $t = 1\,min$), the stabilized voltammogram at 0.1 V s^{-1}, obtained after a few cycles (Fig. 1c), shows a broad pair of conjugated peaks in the same potential region as seen in the blank. In this case, the value of R is about 35 and the total voltammetric charge, Q, remains practically constant during potential cycling between 0.05 and 1.55 V (Fig. 2).

The irreversible voltammetric behaviour of the oxidation–reduction cycles involving surface oxide species as seen through the corresponding peak potential difference at different potential sweep rate, v, is enhanced for RSWP treated specimens (Fig. 3). This behaviour may be due to changes in the oxide surface composition. Both the anodic and the cathodic peak heights increase linearly with v for $v \leqslant 0.1\,V\,s^{-1}$ and change linearly with $v^{1/2}$ for $v \geqslant 0.1\,V\,s^{-1}$ (Fig. 4). At any v, however, the anodic to cathodic peak height ratio is close to about 1.5.

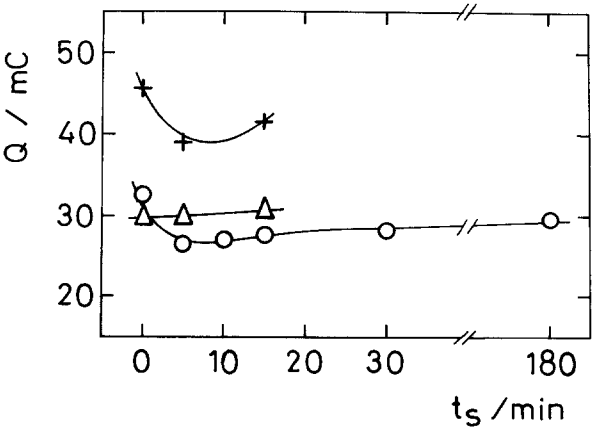

Fig. 2. Dependence of the overall voltammetric charge, Q, for the stabilized electrode after the RSWP treatment ($E_u = 1.0\,V$, $E_l = -1.0\,V$, $t = 1\,min$) on the duration of the potential cycling, t_s, between 0.05 and 1.55 V at 0.1 V s^{-1}, for different RSWP frequencies: (+) 0.6, (△) 0.1 and (○) 1 kHz.

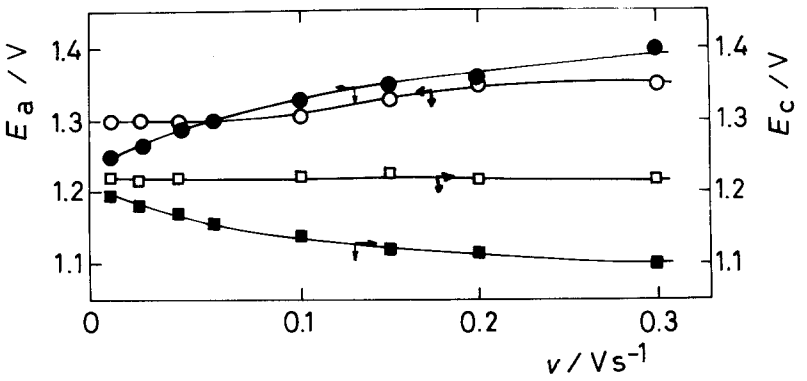

Fig. 3. Dependence of the anodic (E_a) and cathodic (E_c) peak potentials on the potential sweep rate for untreated (○, □) and RSWP treated (●, ■) (E_u = 1.0 V, E_l = −1.0 V, f = 0.6 kHz, t = 1 min) samples.

The anodic to cathodic total voltammetric charge ratio, Q_1/Q_2, (Fig. 5) depends considerably on v below 0.08 V s^{-1}, a fact which has been attributed to either an oxide growth with time, or a partial contribution of o.e.r. to the total charge [11]. But, above 0.1 V s^{-1}, the ratio Q_1/Q_2 approaches the ideally expected value of unity ($\simeq$ 1).

3.2. *Influence of the characteristics of the RSWP*

For a symmetric RSWP (E_l = −1.0 V, f = 2 kHz and t = 1 min), the dependence of R on E_u presents a bell-shaped curve with a maximum at about E_u = 1.0 V (Fig. 6).

Runs made for preset values of f, t and E_u, and E_l changed stepwise show that the greatest value of R is reached at about E_l = −1.0 V (Fig. 7). There is also a threshold E_l value close to −0.8 V. These results are comparable to those reported earlier for pc Ni and Co [20–22]. In all cases, the value of E_l lies in the hydrogen evolution reaction (h.e.r.) potential range.

For RSWP treatment at E_u = 1.0 V, E_l = −1.0 V and t = 1 min the optimal frequency associated with the maximum R value is about 0.6 kHz (Fig. 8).

3.3. *I.r. analysis and X-ray diffractometry*

Oxidized amorphous electrodes were prepared for infrared analysis by applying the RSWP treatment for E_l = −1.0 V, E_u = 1.0 V and f = 0.6 kHz. The oxide powders were then removed, filtered and rinsed with fourfold distilled water.

The 4000–400 cm^{-1} i.r. spectra of the oxide sample exhibit a shoulder at 3640 cm^{-1} which has been assigned to the asymmetric stretching fundamental mode of the 'free' hydroxyl group in $Ni(OH)_2$ (Fig. 9). Bands at 2926, 1461, 1376, 1073, 537 and 432 cm^{-1} [23, 24] are also related to other vibrational modes of $Ni(OH)_2$. The broad adsorption band at 3434 cm^{-1} and the peak at 1640 cm^{-1} are assigned to vibration modes of adsorbed water [25]. The bands located at 2926, 1461, 1376 cm^{-1}, and particularly that at 583 cm^{-1}, can be assigned to cobalt oxides and/or hydroxides [23].

When the oxide powder is treated at 380 °C for 2 h, the i.r. spectra (Fig. 9) show main adsorption bands centred at 662 and 572 cm^{-1}, and a shoulder at

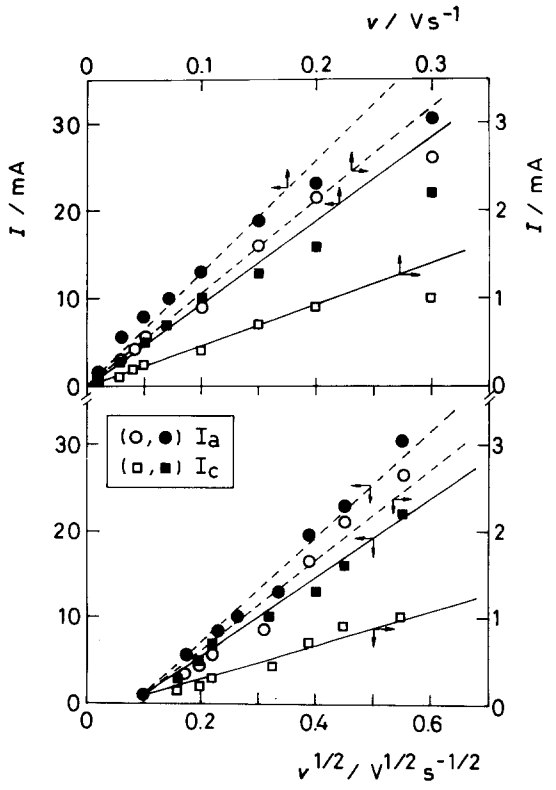

Fig. 4. Dependence of the anodic (I_a) and cathodic (I_c) current peaks for untreated (○, □) and RSWP treated (●, ■) (E_u = 1.0 V, E_l = −1.0 V, f = 0.6 kHz, t = 1 min) samples on the potential sweep rate.

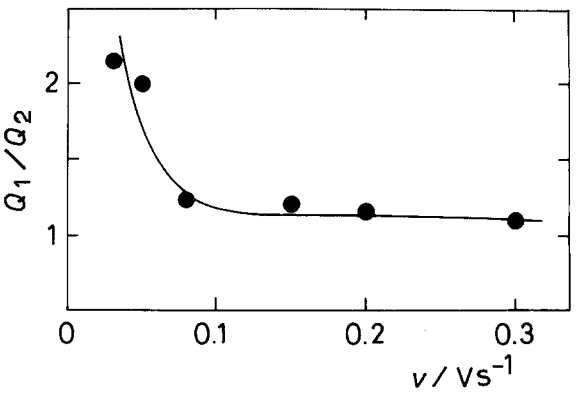

Fig. 5. Dependence of the Q_1/Q_2 ratio for the RSWP treated (E_u = 1.0 V, E_l = −1.0 V, f = 0.6 kHz, t = 1 min) sample on the potential sweep rate.

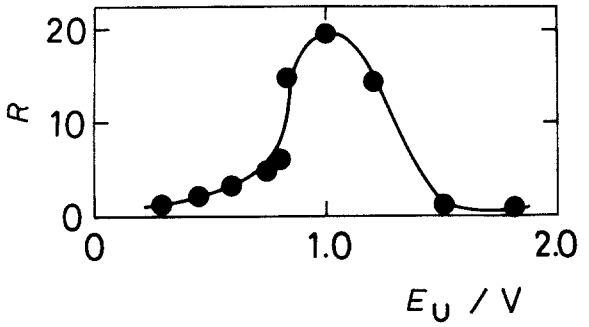

Fig. 6. Dependence of R on E_u for $E_l = -1.0\,V$, $f = 2\,kHz$, $t = 1\,min$.

$390\,cm^{-1}$, which are specific for spinel structures [20, 21, 24, 26].

The X-ray diffraction patterns of the RSWP treated G16 samples show few broad halos, which are particular features for amorphous materials and also for microcrystalline systems, as confirmed for the latter by scanning tunnelling microscopy image [27]. After anodic galvanostatic polarization of a G16 sample in alkaline solution, a nonhomogeneous surface layer was formed consisting of microcrystalline and amorphous domains. The structure of the microcrystalline domains supports the formation of the Co–Ni spinel structure [27].

3.4. *X-ray photoelectron spectroscopy data*

The spectra for Co 2p, Ni 2p and O 1s levels corresponding to the XPS analysis of the bright side of the RSWP treated sample are presented in Fig. 10. The complete XPS data for G16 specimens after chemical etching (ChE) and RSWP treatment are given in Table 1 in terms of binding energies (BE) for both the dull (D) and the bright (B) sides of the metal ribbon. The relative atomic ratios of the different elements at the surface layer are listed in Table 2. The accuracy of these results is within $\pm$ 1 eV. The difference compared to some values reported in the literature can be attributed to insufficient charging correction of the experimental data using surface carbon or to the amorphism of the samples.

The 0 1s peak, located at 530 $\pm$ 1 eV, is typical for transition metal oxides associated with metal–O species. Its slight shift to higher BE, i.e., 531 $\pm$ 1 eV, is specifically observed for hydrous oxides and M–OH species [28].

The Ni $2p^{3/2}$ peak at about 856 eV is related to nickel oxides and suboxides, probably $Ni(OH)_2$ and Ni_2O_3

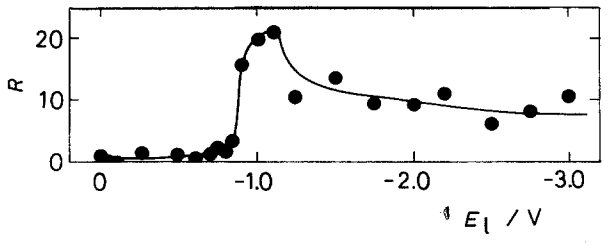

Fig. 7. Dependence of R on E_l for $E_u = 1.0\,V$, $f = 2\,kHz$, $t = 1\,min$.

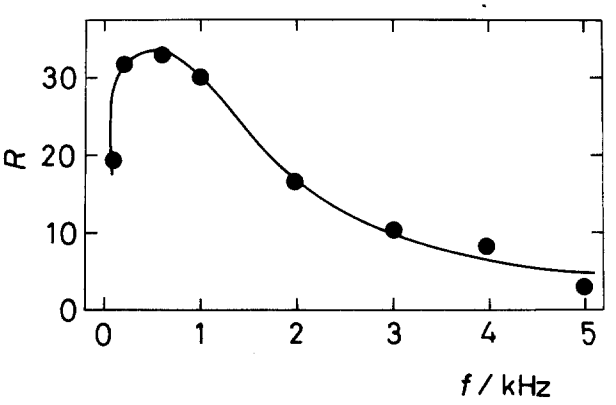

Fig. 8. Dependence of R on f for $E_u = 1.0\,V$, $E_l = -1.0\,V$, $t = 1\,min$.

[28–31]. The definite assignment of the Co $2p^{3/2}$ peak to a particular species is not possible, as it results from the presence of Co_2O_3, CoOOH, CoO, $Co(OH)_2$ and Co_3O_4 [28–30]. Furthermore, for the case of alloys such as G16, the BE of the corresponding components can be displaced $\pm$4 eV [32]. The values of the BE reported in Table 1 are also in agreement with those reported for $NiCo_2O_4$ prepared by thermal decomposition [33].

According to the data in Table 2, as both sides of the working electrode were subjected to the RSWP treatment, an average value for the Ni/Co ratio of 0.5 would correspond to the overall active electrode surface. Likewise, from data of Tables 1 and 2 the average surface composition of the oxide layer formed on G16 after RSWP treatment, can be assigned to different cobalt and nickel hydroxides, such as $[Ni(OH)_2 \cdot 2CoOOH \cdot 6H_2O]$, $[Ni(OH)_2 \cdot 2Co(OH)_2 \cdot 6H_2O]$, $[3Ni(OH)_2 \cdot 2[2CoOOH \cdot Co(OH)_2] \cdot 18H_2O]$, which can be considered as precursors of the $NiCo_2O_4$ formation.

3.5. *OER polarization curves*

The polarization curves for G16 samples in the o.e.r. potential range run at $10^{-4}\,V\,s^{-1}$ are shown in Fig. 11. The values of the current density are referred to the geometrical electrode area. It can be seen that at constant E in the potential range between 1.5 and 1.7 V, the anodic current density corresponding to the RSWP treated sample is always greater than that of the untreated amorphous electrode. At high positive potentials, there is no appreciable difference in the behaviour of both samples since the o.e.r. becomes mass transport controlled.

4. Discussion

The present results demonstrate that the application of the RSWP treatment to the G16 amorphous alloy in alkaline solution promotes the growth of a hydrous oxide film, which behaves as a precursor of a $NiCo_2O_4$ spinel.

The voltammetric behaviour of the RSWP treated amorphous Co–Ni alloy is similar to that of the $NiCo_2O_4$ surface [4, 5, 33]. For freshly prepared

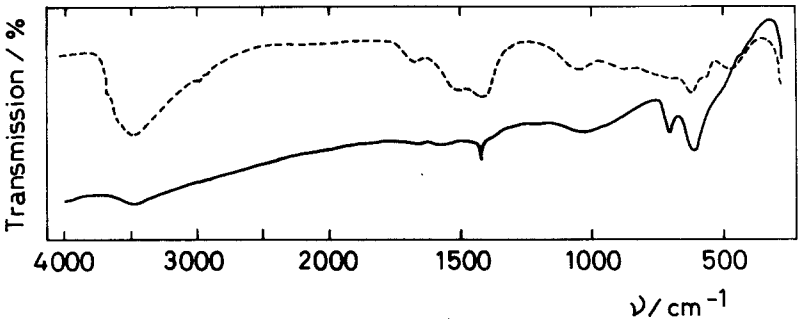

Fig. 9. I.r. spectra for the oxide powders formed by RSWP treatment (E_u = 1.0 V, E_l = −1.0 V, f = 0.6 kHz, t = 1 min), before (- - -) and after (——) thermal treatment at 380 °C during 2 h.

$NiCo_2O_4$ electrodes, Rasiyah *et al.* [4] and Barendrecht *et al.* [33] present voltammograms with two anodic peaks before oxygen evolution and, in the present case, the voltammogram run at 0.1 V s^{-1} immediately after the RSWP treatment (E_u = 1.0 V and E_l = −1.0 V, f = 2 kHz), also exhibits two anodic peaks. According to [4], the peaks may correspond to the transitions: Co(II) ⟶ Co(III), Ni(II) ⟶ Ni(III) and Ni(III) + Co(III) ⟶ Ni(IV) + Co(IV). These higher oxidation states of the metal components of the oxide film appear over a rather wide and high positive potential region (1.25 V ⩽ E ⩽ 1.5 V). On the other hand, Chartier *et al.* [5] present stabilized voltammograms for $NiCo_2O_4$ in the same potential region with only one anodic/cathodic current peak, attributed to the Ni(II)/Ni(III) transition with the participation of Co(III)/Co(IV) species. Barendrecht *et al.* [33] also obtain only one anodic–cathodic current peak after anodic polarization or potential cycling of thermally prepared $NiCo_2O_4$ electrodes.

For Ni–Co alloys the electrochemical formation of oxides was investigated by both cyclic voltammetry and ellipsometry [34]. The formation of a metastable $NiCo_2O_4$ spinel-type oxide by potential cycling was postulated; this decomposes after prolonged oxidation and further behaves as a Co_3O_4 electrode.

In order to explain the high voltammetric reduction charge found for the amorphous alloy G16 as compared with other nickel-containing amorphous alloys, Kreysa *et al.* [14] have proposed the reduction of a $NiCo_2O_4$ spinel-type oxide previously formed by the simultaneous oxidation of cobalt and nickel.

The question as to how a $NiCo_2O_4$ spinel precursor can be grown on a Co–Ni amorphous alloy through the application of the RSWP treatment will now be addressed. The processes occurring in each half cycle during the application of the RSWP to either pc Ni or pc Co electrodes were discussed elsewhere [20–22], and are relevant in explaining the present results. Thus, as the optimal E_u is about 1.0 V, the formation of metal hydroxides involving only the participation of Ni(II) and Co(II) species is favoured. Therefore, the mechanism of the overall process for growing hydrous oxide layers on Co–Ni amorphous alloys can be interpreted through the occurrence of two simultaneous reactions, one involving Ni species and the other Co species.

For the G16 amorphous alloy, the optimal RSWP conditions are 0.7 V ⩽ E_u ⩽ 1.3 V; −1.0 V ⩽ E_l ⩽ −0.9 V and 0.025 kHz ⩽ f ⩽ 2 kHz. These E_u and E_l potential limits related to the maximum value of R are similar to the optimal RSWP potential limits established for pc Ni [20]. For pc Co, the optimal E_u and E_l are located in the net h.e.r. and o.e.r. potential range, respectively. On the other hand, for the present case the value of the optimal frequency is close to that previously determined for RSWP treated pc Co [21]. All these facts may be explained taking into account that for CoNiB glasses it was reported that nickel is the slowly dissolving component [35]. Then, nickel accumulates on the surface, determining the optimal potential limits of the RSWP. However, the optimal frequency to form a spinel precursor is apparently fixed by the cobalt content, which develops oxide layers at lower frequency values than those corresponding to nickel.

For pc Ni subjected to RSWP treatment, a mechanism was proposed which involves the growth of a hydrous nickel(II) hydroxide film during the anodic half-cycle [20], whereas for RSWP treated pc Co the formation of different Co species, namely, $Co(OH)_2$,

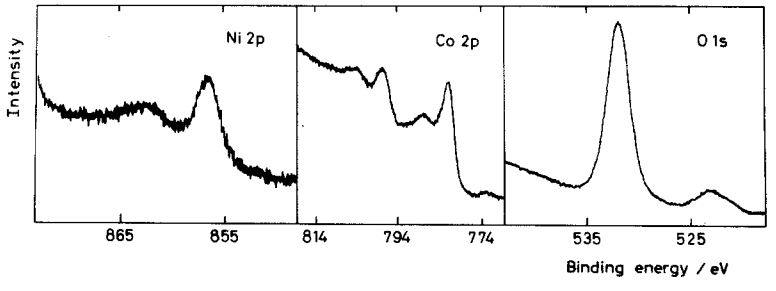

Fig. 10. X-ray photoelectron spectra for Ni 2p, Co 2p and O 1s levels, obtained for a RSWP treated sample (E_u = 1.0 V, E_l = −1.0 V, f = 0.6 kHz, t = 1 min).

Table 1. Binding energies (in eV) for differently treated G16 samples

Sample	*Ni 2p$^{3/2}$*	*Co 2p$^{3/2}$*	*O 1s*
D/ChE	856.8	782.2	532.2
B/ChE	856.8	782.1	532.3
D/RSWP	856.9	781.9	532.4
B/RSWP	857.3	782.2	532.8

CoOOH, CoO_2 was suggested [21, 22]. Furthermore, for pc Ni, as the E_1 is located in the h.e.r. potential range, a local alkalinization is produced during the cathodic half-cycle assisting the formation of $Ni(OH)_2$, but also producing nickel atoms which contribute to the advance in depth of the oxide layer [20]. For pc Co, the metal hydroxide species are partially reduced to Co(o) during the cathodic half-cycle and simultaneously a Co spinel precursor, that is $[Co(OH)_2 \cdot 2CoOOH \cdot 6H_2O]$, is developed [22].

For the present results, the formation of a $NiCo_2O_4$ spinel on the RSWP treated amorphous alloy is also likely. The proposed structure involves the substitution of $Co(OH)_2$ by $Ni(OH)_2$ in the precursor of the cobalt oxide spinel. Such an introduction of nickel ions in place of cobalt ions is possible because of the almost complete isomorphism of the crystal lattices of the cobalt and nickel hydroxides. Furthermore, from the atomic ratio of the components of the oxide layer derived from the XPS data, the most likely average surface composition also corresponds to $[Ni(OH)_2 \cdot 2CoOOH \cdot 6H_2O]$.

Assuming that a spinel oxide film is formed on the amorphous alloy after the RSWP treatment the average film thickness, L, can be estimated through the expression: $L = Q_2 M/Fd$ [36], where M is the molecular weight of the $NiCo_2O_4$ spinel, d is the estimated density of the film ($d \simeq 5.7\,g\,cm^{-3}$) and Q_2 is the cathodic charge obtained from the voltammogram run at $0.1\,V\,s^{-1}$. The estimated average film thickness is about 45 nm, which can be compared with reported data [31] of 4 nm for 'native' dry oxides on an amorphous alloy taking into account that the RSWP treatment produces a highly hydrated oxide layer.

For the o.e.r. the RSWP electroformed oxide layer gives, at constant potential, higher current densities than those of the untreated samples (Fig. 11). For a series of Ni–Co oxides of different composition, the maximum activity towards oxygen evolution, as well as oxygen reduction, was found for the 2Co · Ni composition [37, 38]. This ratio corresponds to that of the $NiCo_2O_4$ spinel which was considered to be the product of substitution of nickel into the spinel oxide

Table 2. Atomic ratios derived from XPS data

Sample	*O/Co*	*Ni/Co*	*O/Ni*
D/ChE	9.55	0.32	29.8
B/ChE	11.24	0.40	28.1
D/RSWP	7.22	0.59	12.2
B/RSWP	6.68	0.38	17.6

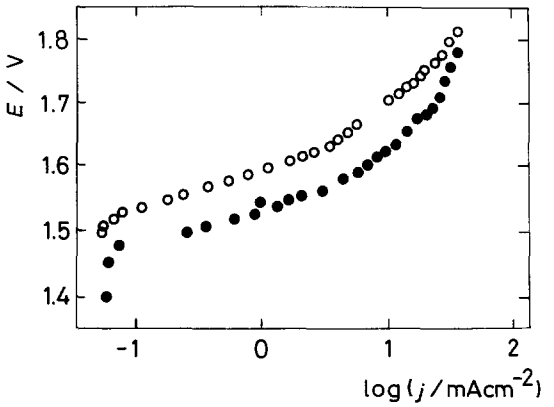

Fig. 11. Tafel plots derived from potentiodynamic runs at $10^{-4}\,V\,s^{-1}$, in 1 M NaOH 30 °C, for G16 electrodes; (○) untreated sample, $R = 1$; (●) RSWP treated sample ($E_u = 1.0\,V$, $E_l = -1.0\,V$, $f = 0.6\,kHz$, $t = 1\,min$), $R \simeq 30$.

Co_3O_4. The maximum permissible amount of cobalt ions which can be substituted by nickel ions in order to maintain the spinel structure was found to be one-third [37]. The distribution of nickel, cobalt and oxygen in the $NiCo_2O_4$ lattice has been extensively discussed and different proposals were put forward [37, 39–42]. Though there is no general agreement, it is likely that the tetrahedral lattice sites are predominantly occupied by Co^{2+} ions and the octahedral ones by Ni^{2+}, Ni^{3+} and Co^{3+} ions [37, 39–42].

Summing up, hydrous oxide films can be grown on Co–Ni amorphous alloys in alkaline solution after the application of a periodic perturbing potential. The electroformed oxide film behaves as a precursor of a Co–Ni spinel as can be inferred from its chemical properties and electrochemical characteristics. The spinel-type structure of the film should be considered as largely responsible for the high catalytic activity of the oxide film for the o.e.r.

Acknowledgements

This research was financially supported by the Consejo Nacional de Investigaciones Científicas y Técnicas. The authors thank Professor G. Kreysa, DECHEMA Institut, Frankfurt/M, for providing the G-16 metal specimens and QUINOR, Facultad de Ciencias Exactas, Universidad Nacional de La Plata, for i.r. spectroscopy measurements. T.K. is a researcher of CIC and Facultad de Ingeniería, Universidad Nacional del Centro de' la Provincia de Buenos Aires, Olavarria (Bs.As.).

References

[1] D. E. Hall, *J. Electrochem. Soc.* **132** (1985) 41 C.
[2] S. Trasatti, IV Simp. Bras. Electroquim. Electroanal. (1984) ANAIS, p. XVII.
[3] J. O'M. Bockris and T. Otagawa, *J. Electrochem. Soc.* **131** (1984) 290.
[4] P. Rasiyah, A. C. C. Tseung and D. B. Hibbert, *ibid.* **129** (1982) 1724.
[5] R. N. Singh, M. Hamdani, J. F. Koening, G. Poillerat, J. L. Gautier and P. Chartier, *J. Appl. Electrochem.* **20** (1990) 442.
[6] M. D. Archer, C. C. Corker and B. H. Harji, *Electrochim. Acta* **32** (1987) 13.

[7] A. Baiker, *Faraday Disc. Chem. Soc.* **87** (1989) 239.
[8] P. C. Searson, P. V. Nagarkar and R. M. Latanision, in 'Modern Aspects of Electrochemistry', Vol. 21, (edited by R. E. White, J. O'M. Bockris and B. E. Conway), Plenum Press, New York (1990), p. 121.
[9] G. A. Tsirlina, O. A. Petrii and N. S. Kopylova, *Elektrokhimiya* **26**(9) (1990) 949.
[10] J. Y. Hout, M. Trudeau, L. Brossard and R. Schulz, *J. Electrochem. Soc.* **136** (1989) 2224.
[11] L. Vračar and B. E. Conway, *Electrochim. Acta* **35** (1990) 1919.
[12] K. Lian, A. N. Kirk and S. Y. Thorpe, *Electrochim. Acta* **36** (1991) 537.
[13] J. J. Podestá, R. C. V. Piatti, A. J. Arvia, P. Ekdunge, K. Jüttner and G. Kreysa, *J. Hyd. Energy*, **17** (1992) 9.
[14] G. Kreysa and B. Hakansson, *J. Electroanal. Chem.* **201** (1986) 61.
[15] H. Alemu and K. Jüttner, *Electrochim. Acta* **32** (1988) 1101.
[16] T. Kessler, J. R. Vilche, M. Elbert, K. Jüttner and W. J. Lorenz, *Chem. Eng. Technol.* **14** (1991) 263.
[17] K. K. Lian and V. I. Birss, *J. Electrochem. Soc.* **138** (1991) 2885.
[18] L. D. Burke and D. P. Whelan, *J. Electroanal. Chem.* **109** (1980) 385.
[19] L. D. Burke, M. E. Lyons and O. J. Murphy, *ibid.* **132** (1982) 247.
[20] A. Visintin, A. C. Chialvo, W. E. Triaca and A. J. Arvia, *ibid.* **225** (1987) 227.
[21] T. Kessler, M. R. G. de Chialvo, A. Visintin, W. E. Triaca and A. J. Arvia, *ibid.* **261** (1989) 315.
[22] T. Kessler, A. Visintin, W. E. Triaca, A. J. Arvia and M. R. G. de Chialvo, *J. Appl. Electrochem.* **21** (1991) 516.
[23] "The Sadtler Standard Spectra", Sadtler Research Lab. Inc., Philadelphia (1967).
[24] I. S. Shamina, O. G. Maladin, S. M. Rakowskayaa, L. N. Sal'kova, A. V. Vasev and A. Vereshchagina, *Elektrokhimiya* **12** (1976) 573.
[25] U. Z. Barsukov, L. N. Sagoyan, N. R. Meshcheryakova and A. G. Gerasimov, *ibid.* **21**(1) (1985) 17.
[26] J. Preudhomme and P. Tarte, *Spectrochim. Acta* **27A** (1971) 1817.
[27] G. Kreysa, J. Gómez Baró and A. J. Arvia, *J. Electroanal. Chem.* **265** (1989) 67.
[28] N. S. McIntyre and M. G. Cook, *Anal. Chem.* **47** (1975) 2208.
[29] R. B. Diegle, N. R. Sorensen, C. R. Clayton, M. A. Helfond and J. C. Yu, *J. Electrochem. Soc.* **135** (1988) 1085.
[30] D. Majumdar, R. G. Spahn and J. S. Gau, *ibid.* **134** (1987) 1825.
[31] P. V. Nagarkar, S. K. Kulkarni and E. Umbach, *Appl. Surf. Sci.* **29** (1987) 194.
[32] N. H. Turner and R. J. Colton, *Anal. Chem.* **54** (1982) 294R.
[33] J. Haenen, W. Visscher and E. Barendrecht, *J. Electroanal. Chem.* **208** (1986) 273, 297, 323.
[34] J. Haenen, W. Nisscher and E. Barendrecht, *Electrochim. Acta* **31** (1986) 1541.
[35] K. E. Heusler and D. Huerta, *J. Electrochem. Soc.* **136** (1989) 65.
[36] R. E. Carbonio, V. A. Macagno, M. C. Giordano, J. R. Vilche and A. J. Arvia, *ibid.* **129** (1982) 983.
[37] W. J. King and A. C. C. Tseung, *Electrochim. Acta* **19** (1974) 485.
[38] A. C. C. Tseung and S. M. Jasem, *ibid.* **22** (1977) 31.
[39] F. K. Lotgering, *Philips Res. Rep.* **11** (1956) 337.
[40] G. Blasse, *ibid.* **18** (1963) 383.
[41] J. O. Knop, K. I. Reid, Saturno et Y. Nakagawa, *Can. J. Chem.* **46** (1968) 3463.
[42] M. Hamdani, J. F. Koening and P. Chartier, *J. Appl. Electrochem.* **18** (1988) 561.